Near Real-Time Fuel-Optimal En Route Conflict Resolution

Adan E. Vela, Senay Solak, John-Paul B. Clarke, William E. Singhose, Earl R. Barnes, and Ellis L. Johnson

***Abstract*—In this paper, we consider the air-traffic conflict-resolution problem and develop an optimization model to identify the required heading and speed changes of aircraft to avoid conflict such that fuel costs are minimized. Nonconvex fuel functions in the optimization problem are modeled through tight linear approximations, which enable the formulation of the problem as a mixed-integer linear program. The significance of the developed model is that fuel-optimal conflict-resolution maneuvers can be identified in near real time, even for conflicts involving a large number of aircraft. Computational tests based on realistic air-traffic scenarios demonstrate that conflicts involving up to 15 aircraft can be solved in less than 10 s with an optimality gap of around 0.02%.**

***Index Terms*—Air-traffic control, conflict resolution, integer programming.**

I. Introduction

THE DEVELOPMENT of advanced air-traffic conflict-detection and resolution algorithms is important to the overall improvement of the air-traffic management (ATM) system. This is particularly true when one considers issues of safety and capacity within the context of growing air traffic.

A conflict in air traffic occurs when two or more aircraft encroach upon the minimum required separation, as defined by the regulator. Conflict detection is the identification of potential conflicts through prediction of future aircraft trajectories based on their current positions, headings, and flight plans. Once a conflict is detected, it is resolved by changing the trajectory of one or more aircraft so that the minimum separation requirements are satisfied.

Aircraft conflict detection and resolution have been studied extensively. A comprehensive survey of the proposed models is presented in [1]. Since the publication of that survey, several other methods have been introduced, as automated conflict resolution has been proposed as an important component of the next-generation air-traffic control system. Emphasizing this fact, Erzberger [2] and Farley *et al.* [3] describe a multiphase procedure to resolve pairwise conflicts and present computational studies for forecasted future traffic levels, including merging arrivals. The approaches developed over the past few years include a 3-D model based on a collision cone approach [4], where the solution of the model requires significant computational effort. Another computationally intensive approach, which is suggested in [5], requires the identification of all conflict-free maneuvers and then the selection of the best such maneuver. In [6], a geometric optimization procedure for conflict avoidance and recovery is described.

In other recent studies, Mondoloni and Conway [7] and Vivona *et al.* [8] suggest genetic algorithm approaches based on a predefined set of maneuvers for aircraft. Idris *et al.* [9] describe a time-based conflict-resolution algorithm, where the resolution is achieved by time delaying or advancing one of the aircraft involved in the conflict. Furthermore, Kirk *et al.* [10] describe a function that is termed problem analysis, resolution, and ranking, which provides a set of candidate conflict-resolution advisories to the controller. The resolution is achieved by testing and ranking the effectiveness of a predetermined set of maneuvers in all three dimensions. However, only one aircraft is maneuvered for each resolution, which typically results in suboptimal solutions. Other conflict-resolution approaches involve a kinematic optimal control model [11], a cooperative multiagent negotiation technique [12], and a hybrid system model that generates safe maneuvers for aircraft [13].

Three recent conflict-resolution models are directly related to the approach described in this paper. These methods contain integer programming models, which enable relatively fast calculations of an optimal conflict-resolution procedure. In the first study [14], two integer programming models are developed by allowing all aircraft to perform either speed changes or heading changes, but not both. The objective of the conflict resolution algorithm is defined as the minimization of the maximum deviation of the changes made. In the second study [15], a similar integer programming model that also accounts for controller workload is discussed. However, the model assumes that only heading changes are allowed to resolve conflict. A third approach [16] considers the problem in three dimensions and solves for a resolution with only velocity changes using a nonlinear integer programming model, which requires a high level of computational effort.

Manuscript received September 13, 2007; revised May 24, 2008, June 29, 2009, and March 21, 2010; accepted May 10, 2010. Date of publication July 8, 2010; date of current version December 3, 2010. This work was supported in part by the Partnership for Air Transportation Noise and Emissions Reduction under Federal Aviation Administration Contract 05-C-NE-GIT-4 and in part by the National Aeronautics and Space Administration under Contract NNA06CN31A. The Associate Editor for this paper was F.-Y. Wang.

A. E. Vela and W. E. Singhose are with the School of Mechanical Engineering, Georgia Institute of Technology, Atlanta, GA 30332 USA (e-mail: aevela@gatech.edu).

S. Solak is with the Finance and Operations Management Department, Isenberg School of Management, University of Massachusetts, Amherst, MA 01003 USA.

J.-P. B. Clarke is with the School of Aerospace Engineering, Georgia Institute of Technology, Atlanta, GA 30332 USA.

E. R. Barnes and E. L. Johnson are with the School of Industrial and Systems Engineering, Georgia Institute of Technology, Atlanta, GA 30332 USA.

Color versions of one or more of the figures in this paper are available online at http://ieeexplore.ieee.org.

Digital Object Identifier 10.1109/TITS.2010.2051028

In this paper, we significantly extend these ideas to a more general case where both heading and speed changes are allowed and where more complex objectives are considered, including minimization of the fuel costs required to return to the desired flight path after a heading change.

In [1], the existing conflict detection and resolution methods are characterized according to scope, dimensions, resolution methodology, and maneuvers. Following this categorization, our proposed approach is a global conflict-resolution procedure for all aircraft that are involved in a conflict. Although the conflict-resolution procedure is described in the horizontal plane only, adaptation to vertical planes is possible by modeling multiple horizontal layers and introducing variables to account for transitions between these layers. This extension, which we further detail in Section VII, is likely to add further value to the algorithm, as altitude adjustments can be the preferred strategy for many conflict scenarios.

The developed mathematical model provides a broad framework for resolving conflicts through fast numerical optimization methods and allows for both heading and speed changes. Particular focus has been placed on reducing fuel costs involved in conflict resolution. This was deemed to be important given the significant role that fuel plays in the operating cost of aircraft and the growing concern regarding the impact of gaseous emissions on the environment. Another significant aspect of the proposed approach is the ability to solve a complex problem in near real time for conflicts involving a large number of aircraft.

There have been two general types of approaches in the existing conflict-resolution studies: rule-based and optimization-based methods. The biggest advantage of rule-based approaches over those that use mathematical optimization techniques has been that they can be implemented in real time without significant computational effort. Hence, the applicability of optimization methods in conflict resolution has been limited. In this paper, we remedy that shortcoming by developing a valid model that can be implemented to resolve conflicts in near real time. In addition to real-time implementations, the proposed model can be used within test and simulation environments for air-traffic control, such as in capacity calculations of sectors or in studies of the free flight concept.

In Section II, we provide a general description of the problem. In Section III, we describe the modeling of the separation constraints that are required for conflict resolution. In Section IV, linear approximations of the complex fuel-cost structures are discussed, while in Section V, we provide a summary of the formulation of the problem. In Section VI, we present the results of the computational studies that are performed, and in Section VII, we present our conclusions.

II. Problem Description

Consider a set of n aircraft located in a Euclidean plane. Each aircraft i is defined by an initial position $\mathbf{p}_i = (x_i, y_i)$, a velocity vector $\mathbf{v}_i^0 = (v_{i,x}^0, v_{i,y}^0)$ defining speed and heading, and a desired final heading θ_i^d. This initial state assumption is not restrictive for en route travel, as the vast majority of en route travel is dominated by steady-state cruising of aircraft.

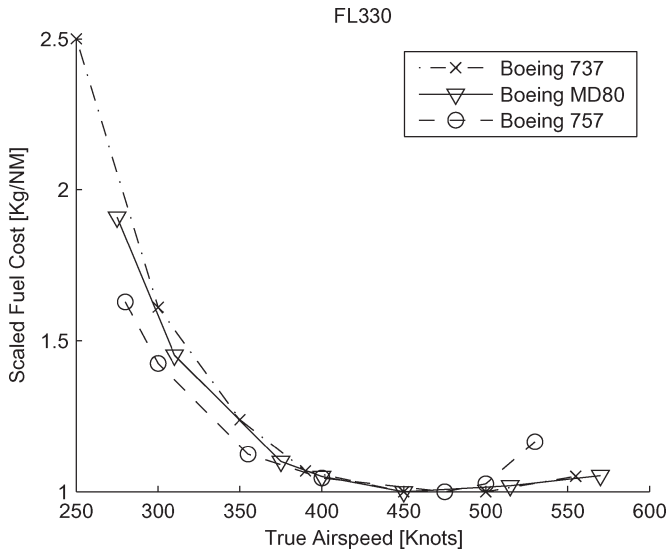

Fig. 1. Sample fuel burn curves for three different aircraft models at FL330 [17].

Even when focusing on maneuvers—speed changes, heading changes, and altitude changes—the time scale for which these occur is insignificant compared with the time to conflict and, hence, can be approximated as occurring instantaneously. Furthermore, en route aircraft typically limit speed and heading changes to small values to ensure that flight plan amendments are not required. In addition, altitude changes are typically restricted to climbing or descending a single flight level due to significant fuel costs. Hence, when considering the time to conflict in common en route traffic and the time to implement conflict maneuvers, the corresponding time scale allows for the reasonable assumption that aircraft maneuvers occur instantaneously and, thus, do not require consideration of all possible initial states.

All aircraft in the problem are designated to be a particular model type with corresponding fuel burn characteristics for the given altitude. Sample "fuel burn curves" at 33 000 ft (FL330) for three different types of aircraft are shown in Fig. 1, based on data obtained from [17]. In this plot, fuel costs are scaled such that a value of 1 corresponds to the minimum fuel burn for the given aircraft type and flight level. The primary task is to assign each aircraft a single instantaneous heading and speed change at $t = 0$ that provides conflict-free travel, while minimizing a measure of the fuel burn costs over all the aircraft trajectories.

The trajectory of any aircraft i is deemed to be conflict-free if the distance between aircraft i and any other aircraft j, i.e., $d_{i,j} = d_{j,i}$, will always be greater than the minimum distance of $d_{i,j}^{\min}$. For the purpose of commercial air travel, the nominal minimum separation distance $d = d_{i,j}^{\min}$ between aircraft is 5 nmi for all aircraft. The minimum separation distance can be visualized by encircling each aircraft with a safety region of radius $d/2$, as shown in Fig. 2. If we assume that trajectories of aircraft are linearly extrapolated in time, then for aircraft i and j with given trajectories, the necessary minimum separation condition is expressed by the following inequality:

$$\sqrt{x_{\text{dist}}^2 + y_{\text{dist}}^2} \geq d \qquad \forall\, t \in R^+ \tag{1}$$

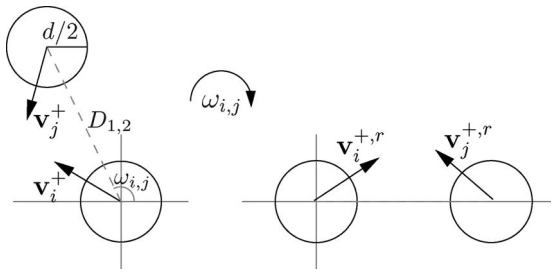

Fig. 2. To prevent singularities, all pairs of planes are rotated.

where x_{dist} and y_{dist} represent the distance between the two aircraft in the corresponding coordinate axes, i.e.,

$$\begin{aligned} x_{\text{dist}} &= (x_i + v_{i,x}t) - (x_j + v_{j,x}t) \\ y_{\text{dist}} &= (y_i + v_{i,y}t) - (y_j + v_{j,y}t). \end{aligned} \tag{2}$$

Over the next few sections, we describe a methodology for formulating a fuel-optimal conflict-resolution model that ensures that separation condition (1) holds for $t \in R^+$. Unlike most models in the literature, the process yields a mixed-integer linear programming problem, which is solvable in near real time for dynamic routing decisions.

Before describing the details of the proposed approach, we first list some initialization assumptions. We assume that no aircraft violate the minimum separation condition (1) at $t = 0$. Also, no initial conditions are such that aircraft are on a collision course that cannot be avoided with control actions over a reasonable time frame. The model does not take into account the time to execute state changes. It is assumed that deviations are small, and the time to complete any maneuver change is small in comparison to the time until conflict. However, the safety region about each aircraft can be expanded to handle uncertainty from resulting maneuver changes, wind variation, or other unmodeled phenomena. Another possible approach could be to include probabilistic constraints and utilize stochastic optimization procedures. However, such models significantly suffer from the curse of dimensionality, and only very small and impractical instances are solvable for problems of this type. Similar issues also occur with deterministic models that try to capture stochasticity through the consideration of growing regions of uncertainty, as discussed in [18].

Considering that the proposed procedure in this paper is a fast and efficient algorithm that is capable of solving problems with a large number of aircraft, and the observation that the time to complete a maneuver is small in comparison to the time until conflict, it is reasonable to assume that any necessary adjustments to compensate for random phenomena will be minor and practically implementable by air-traffic controllers. On the other hand, if the separation distance is increased, no such adjustments will be necessary.

Starting with the initial conditions $\{(\mathbf{p}_i, \mathbf{v}_i^0)\}$, the solution to the resulting optimization model will be the set of new velocity vectors $\{\mathbf{v}_i^+\}$ for each aircraft. Updated speed and heading commands can then be extracted from $\mathbf{v}_i^+$. The new velocity vector $\mathbf{v}_i^+$ represents the solution for an instantaneous change in the trajectory.

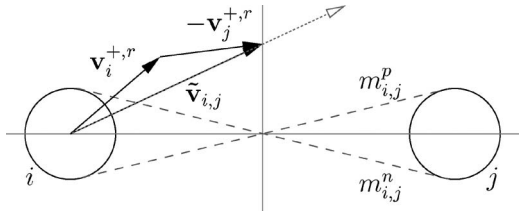

Fig. 3. Definition of the safety regions for aircraft.

III. Separation Constraints

For conflict-free trajectories, each pair of aircraft must satisfy separation constraint (1). Here, the separation condition is deconstructed into a set of linear constraints that ensure no aircraft encroaches another aircraft's safety region. This approach is similar to the one used in [14] to determine the separation constraints.

Consider a pair of aircraft i and j with initial position and velocity states

$$\begin{aligned} \mathbf{p}_i &= (x_i, y_i) \quad \mathbf{v}_i^0 = \left[v_{i,x}^0, v_{i,y}^0\right]^T \\ \mathbf{p}_j &= (x_j, y_j) \quad \mathbf{v}_j^0 = \left[v_{j,x}^0, v_{j,y}^0\right]^T. \end{aligned} \tag{3}$$

A given aircraft i may alter its trajectory to prevent conflict by changing its velocity vector by $\mathbf{dv}_i = [dv_{i,x}, dv_{i,y}]^T$. Applying $\mathbf{dv}_i$ to each corresponding aircraft defines new trajectories as follows:

$$\mathbf{v}_i^+ = \mathbf{v}_i^0 + \mathbf{dv}_i \quad \mathbf{v}_j^+ = \mathbf{v}_j^0 + \mathbf{dv}_j. \tag{4}$$

To avoid singularities in the problem formulation, the reference frame for the pair of planes is rotated so that the angle $\omega_{i,j} = 0$, where $\omega_{i,j}$ is the angle between the horizon and the connector between the aircraft. This process is demonstrated in Fig. 2. For an initial angle $\omega_{i,j} \in [0, 2\pi)$, rotation is performed by multiplying the initial position and velocity vectors by the rotation matrix $\mathbf{R}(\omega_{i,j})$, i.e.,

$$\begin{aligned} \mathbf{R}(\omega_{i,j}) &= \begin{bmatrix} \cos(\omega_{i,j}) & \sin(\omega_{i,j}) \\ -\sin(\omega_{i,j}) & \cos(\omega_{i,j}) \end{bmatrix} \\ \mathbf{p}_i^r &= \mathbf{R}(\omega_{i,j})(x_i, y_i), \quad \mathbf{v}_i^{+,r} = \mathbf{R}(\omega_{i,j})\mathbf{v}_i^+ \\ \mathbf{p}_j^r &= \mathbf{R}(\omega_{i,j})(x_j, y_j), \quad \mathbf{v}_j^{+,r} = \mathbf{R}(\omega_{i,j})\mathbf{v}_j^+. \end{aligned} \tag{5}$$

Once the rotation is performed, a set of linear constraints to ensure that a pair of aircraft maintain separation is derived from the relative velocity $\tilde{\mathbf{v}}_{i,j}$ and the initial position $\tilde{\mathbf{p}}_{i,j}$ of aircraft i and j, i.e.,

$$\begin{aligned} \tilde{\mathbf{v}}_{i,j} &= \mathbf{v}_i^{+,r} - \mathbf{v}_j^{+,r} \\ \tilde{\mathbf{p}}_{i,j} &= \mathbf{p}_i^{+,r} - \mathbf{p}_j^{+,r}. \end{aligned} \tag{6}$$

Conflict between aircraft i and j occurs when the ray originating from aircraft i extending along $\tilde{\mathbf{v}}_{i,j}$ passes through aircraft j. To ensure separation, an implementation based on the definition of a safety region around each aircraft is possible. For aircraft with safety regions of radius $d/2$, the projected safety region of aircraft i along $\tilde{\mathbf{v}}_{i,j}$ must remain outside the safety region of aircraft j, as illustrated in Fig. 3.

By understanding the method of ray extension along the relative velocity, the allowable regions for $\tilde{\mathbf{v}}_{i,j}$ can be delineated. Ultimately, the set of crossing lines $l^p_{i,j}$ and $l^n_{i,j}$, with slopes $m^p_{i,j}$ and $m^n_{i,j}$, tangent to the safety regions of each aircraft is key to defining the linear constraints through the following relation:

$$\begin{aligned} &\frac{\tilde{v}_{i,j,y}}{\tilde{v}_{i,j,x}} \leq m^n_{i,j} \\ \text{or} \quad &\frac{\tilde{v}_{i,j,y}}{\tilde{v}_{i,j,x}} \geq m^p_{i,j}. \end{aligned} \tag{7}$$

For aircraft that are D distance apart, with mandatory separation d, the slopes $m^p_{i,j}$ and $m^n_{i,j}$ are given by

$$\begin{aligned} m^p_{i,j} &= d/\sqrt{D^2 - d^2} \\ m^n_{i,j} &= -d/\sqrt{D^2 - d^2}. \end{aligned} \tag{8}$$

Constraints (7) can be expressed as linear inequalities by multiplying the right-hand side by the denominator $\tilde{v}_{i,j,x}$. Enforcing the condition $\tilde{v}_{i,j,x} \leq 0$, separation is then ensured when

$$\begin{aligned} &\tilde{v}_{i,j,y} \leq \tilde{v}_{i,j,x} m^n_{i,j}, && \tilde{v}_{i,j,x} \geq 0 \\ \text{or} \quad &\tilde{v}_{i,j,y} \geq \tilde{v}_{i,j,x} m^n_{i,j}, && \tilde{v}_{i,j,x} \leq 0 \\ \text{or} \quad &\tilde{v}_{i,j,y} \geq \tilde{v}_{i,j,x} m^p_{i,j}, && \tilde{v}_{i,j,x} \geq 0 \\ \text{or} \quad &\tilde{v}_{i,j,y} \leq \tilde{v}_{i,j,x} m^p_{i,j}, && \tilde{v}_{i,j,x} \leq 0. \end{aligned} \tag{9}$$

Removing overlaps in conditions (9), the constraints are reduced to

$$\begin{aligned} &\tilde{v}_{i,j,y} \leq \tilde{v}_{i,j,x} m^n_{i,j}, && \tilde{v}_{i,j,x} \geq 0 \\ \text{or} \quad &\tilde{v}_{i,j,y} \geq \tilde{v}_{i,j,x} m^p_{i,j}, && \tilde{v}_{i,j,x} \geq 0 \\ \text{or} \quad &\tilde{v}_{i,j,x} \leq 0. \end{aligned} \tag{10}$$

The separation constraints (10) are expressed as linear inequalities of the decision variables $\tilde{v}_{i,j,x}$ and $\tilde{v}_{i,j,y}$, which are functions of the speed and heading changes $\mathbf{dv}_i$. Furthermore, the condition $\tilde{v}_{i,j,x} \leq 0$ allows for the case of aircraft trailing one another, i.e., the singularity of $\tilde{v}_{i,j,x} = 0$ in the slope is admissible for this formulation. The constraints (10) are then applied to all pairs of aircraft. As the constraints are reciprocal, only one set of constraints is required for each pair, i.e.,

$$\begin{aligned} &\tilde{v}_{i,j,y} \leq \tilde{v}_{i,j,x} m^n_{i,j}, && \tilde{v}_{i,j,x} \geq 0 \\ \Leftrightarrow \quad &\tilde{v}_{j,i,y} \leq \tilde{v}_{j,i,x} m^n_{j,i}, && \tilde{v}_{j,i,x} \geq 0 \\ &\tilde{v}_{i,j,y} \geq \tilde{v}_{i,j,x} m^p_{i,j}, && \tilde{v}_{i,j,x} \geq 0 \\ \Leftrightarrow \quad &\tilde{v}_{j,i,y} \geq \tilde{v}_{j,i,x} m^p_{j,i}, && \tilde{v}_{j,i,x} \geq 0 \\ &\tilde{v}_{i,j,x} \leq 0 \\ \Leftrightarrow \quad &\tilde{v}_{j,i,x} \leq 0. \end{aligned} \tag{11}$$

Because all pairs of aircraft are resolved simultaneously for all future time, there are no secondary conflicts.

A detailed derivation of these separation constraints is described in the Appendix. Note that if avoidance is required to route an aircraft around a no-fly region, moving weather formation, or any type of obstacle, then the same process can be used to form the set of linear constraints. For a nonmoving obstacle, it is assumed that $\mathbf{dv}_{\text{obs}} = 0$. The slopes for $l^p_{i,\text{obs}}$ and $l^n_{i,\text{obs}}$ are given by $m^p_{i,\text{obs}} = (d + d_{\text{obs}})/2D$ and $m^n_{i,\text{obs}} = -(d + d_{\text{obs}})/2D$, where d_{obs} can be selected as the diameter of the smallest circle encircling the obstacle.

IV. Cost Formulation

In line with the primary goal of providing a framework in which fuel costs are considered in conflict resolution and aircraft routing, an appropriate cost function $G_0(\mathbf{s}, \theta)$ can be defined as

$$G_0(\mathbf{s}, \boldsymbol{\theta}) = g_s(\mathbf{s}) + g_h(\boldsymbol{\theta}) \tag{12}$$

where g_s and g_h are nonlinear scalar functions of the airspeeds $\mathbf{s}$ and the headings θ of the aircraft. The function g_s measures the fuel burn percentage of an aircraft, while g_h accounts for the scaled increase in distance traveled due to a deviation from the desired route and the estimated cost to return to the desired path. Considering both parts, G_0 is the fuel-consumption percentage with respect to the optimal path at a desired airspeed when there are no obstacles. In other words, the cost function considers the percent increase in fuel cost for each aircraft over the optimal fuel-consumption rate when no other aircraft, weather, or other blockages are considered. The percent increase in cost is a result of heading changes that increase travel distance or speed changes that may force aircraft to operate at suboptimal airspeeds. Hence, under the assumptions of the model, the calculated costs for an optimal solution correspond to the lowest possible total cost required to resolve conflicts for the set of flights considered.

The measures $\mathbf{s}$ and θ, and, thus, the cost functions $g_s(\mathbf{s})$ and $g_h(\theta)$, are nonlinear nonconvex functions of the decision variables $\mathbf{dv}_i$. In the following, we develop tight convex linear approximations for these functions and show that the underlying optimization problem can be modeled as a linear integer-programming problem.

A. Fuel Costs Due to Change in Airspeed

Previous conflict-resolution research described in Section I focused on minimizing the velocity deviation $\mathbf{dv}_i$ that an aircraft is required to make to ensure separation. Noting that any such deviation incurs costs, a measure of airspeed is required to provide a broader framework to understand and study the fairness and the costs associated with aircraft routing. The final airspeed of aircraft i, i.e., s^+_i, for determination of fuel burn can be calculated according to a first-order approximation, i.e.,

$$s^+_i \sim s^0_i + \frac{1}{s^0_i}\left[v^0_{i,x} v^0_{i,y}\right] \mathbf{dv}_i = \hat{s}_i. \tag{13}$$

While a first-order approximation is satisfactory for $\mathbf{dv}_i$ when $\|\mathbf{dv}_i \times \mathbf{v}^0_i\| \sim 0$, the approximation deteriorates as larger heading angle changes are required to avoid conflicts. Assuming an aircraft is operating near its optimal fuel burn speed, the percent error in airspeed arising from the use of approximation (13) is shown in Fig. 4. For heading deviations of 15° and greater, this error diminishes the ability of any formulation to utilize this approximation to effectively solve for fuel-optimal routing.

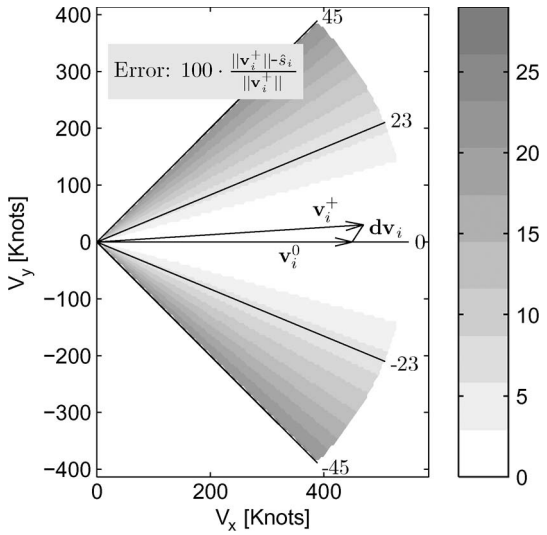

Fig. 4. Percent error in the first-order approximation of airspeed.

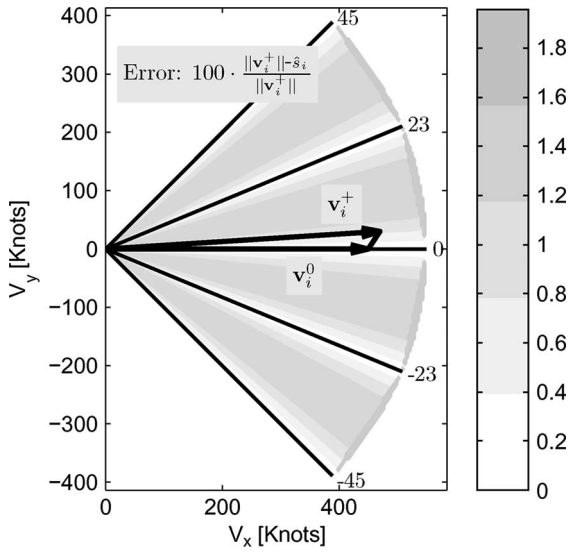

Fig. 5. Percent error in the SOS2 approximation of airspeed.

To overcome the shortcomings that are associated with a first-order approximation, additional constraints that make use of special ordered sets of type 2 (SOS2) can be utilized to provide a more accurate approximation of airspeed. SOS2 variables are a set of nonnegative continuous variables such that, at most, one pair of consecutively indexed variables is nonzero. Hence, if $\lambda_1, \ldots, \lambda_n$ is SOS2, and if $\lambda_i \geq 0$, then either $\lambda_{i-1} \geq 0$ or $\lambda_{i+1} \geq 0$ and all other $\lambda_j = 0$. Although introduction of SOS2 variables into the optimization model, which we describe in detail below, adds to the complexity of the formulation, it enables a much better approximation of the airspeed over the feasible region.

Consider an aircraft with some initial heading θ^0, and which can perform heading changes of $\pm d\theta$ to ensure separation, consistent with typical ATM procedures. We assume that the range of possible final heading values is broken into m adjacent regions according to the set $\theta = \{d\theta_1 + \theta^0, \ldots, \theta^0, \ldots, d\theta_m + \theta^0\} = \{\theta_1, \ldots, \theta_m\}$. These regions need not be uniform in size. A grid structure over the feasible space is then formed, including the origin and the set $(X_q, Y_q) = \{v_i^{\max}\cos(\theta_q), v_i^{\max}\sin(\theta_q)\}, \ \forall\, q \in \{1, 2, \ldots, m\}$. The function $Z_q = \|\mathbf{v}_q\|$ is then evaluated over the grid points. The airspeed $\hat{s}_i$ is calculated by forming a convex combination of the function values of the grid points that are associated with the sector encompassing $\mathbf{v}_i^+$. The airspeed is given by the following set of constraints:

$$\hat{v}_{i,x}^+ = \sum_{q=0}^{m} X_q \lambda_q$$

$$\hat{v}_{i,y}^+ = \sum_{q=0}^{m} Y_q \lambda_q$$

$$\hat{s}_i = \sum_{q=0}^{m} Z_q \lambda_q$$

$$\sum_{q=0}^{m} \lambda_q = 1, \qquad \lambda_q \in \text{SOS2} \qquad \forall\, q. \tag{14}$$

The SOS2 approximation yields a much tighter approximation over the domain, as shown in Fig. 5. For the example provided, even with only four regions, spread over $\pm 45^\circ$ around the initial heading, the largest percent error between the approximation and the actual airspeed is only 2%. In comparison, the linear approximation in (13) increases with the heading change, reaching an error of approximately 30% at 45°.

For the SOS2 case presented above, zero-wind condition is assumed; however, the values of (X_q, Y_q) can be adjusted such that they take into head or tail winds in any direction.

The implementation of SOS2 variables over the range $\theta^0 \pm d\theta$ for each aircraft implicitly defines constraints on the magnitude of any heading changes. These constraints can be defined to be consistent with standard turning performance parameters of the aircraft. Furthermore, it is possible to impose constraints on the airspeed of aircraft through the inclusion of the following constraint:

$$\hat{s}_i^{\min} \leq \hat{s}_i \leq \hat{s}_i^{\max} \tag{15}$$

where $\hat{s}_i^{\min}$ and $\hat{s}_i^{\max}$ are the minimum and maximum airspeeds for the ith aircraft, respectively. However, this constraint, while possible, is not included in the formulation. Simulation results demonstrate that allowing for heading changes and penalizing suboptimal airspeeds through the cost function are sufficient in preventing aircraft from operating at excessively slow or fast airspeeds.

For cost calculations due to airspeed changes, we assume that the airspeed cost for each aircraft is the percent deviation in fuel burn per unit distance traveled when compared with the optimal speed of the aircraft. Given the fuel burn per minute as a function of the true airspeed, this value can be converted to fuel burn per nautical mile traveled by dividing by the ground speed.

Assuming a diverse set of aircraft models, it is important to consider the fuel burn equations for each model type. For each aircraft model, we define a set of l linear inequalities defined by slopes $a_{k,i}$ and intercepts $b_{k,i}$ for $k = 1, \ldots, l$, based on fuel

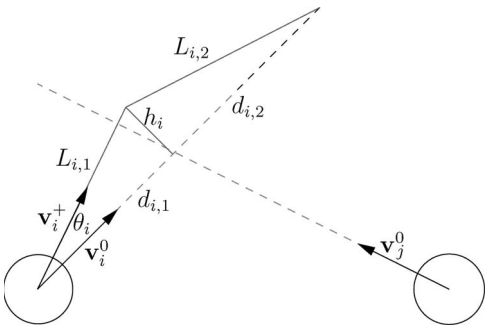

Fig. 6. Heading angle deviations increase the resulting distance traveled as calculated by $L_{i,1} + L_{i,2}$.

curves such as the ones in Fig. 1. These inequalities are then used to formulate the approximate convex fuel cost t_i for the ith aircraft, i.e.,

$$\begin{aligned} a_{1,i}\hat{s}_i + b_{1,i} &\le t_i \\ a_{2,i}\hat{s}_i + b_{2,i} &\le t_i \\ &\vdots \\ a_{l,i}\hat{s}_i + b_{l,i} &\le t_i. \end{aligned} \tag{16}$$

B. Fuel Costs Due to Change in the Heading Angle

The fuel cost associated with a heading angle deviation and a return to the desired flight path is approximated using a two-step process that is illustrated in Fig. 6. In the first step, the aircraft makes a heading change to resolve conflict and travels for a distance of $L_{i,1}$. In the second stage, after the conflict is cleared, the heading is corrected back toward the destination. The travel distance to the destination with this corrected heading is denoted by $L_{i,2}$. In conjunction with conflict detection methods, we assume that there exists complete knowledge of the system. Particularly, we assume that conflict detection methods can predict the largest distance $d_{i,1}$ for a possible conflict between aircraft i with another aircraft assuming that no corrective action is taken, where $d_{i,1}$ is described in Fig. 6. Let $D_i = d_{i,1} + d_{i,2}$ designate the straight-line distance between the destination and the current position of the airplane i. If maintaining separation requires a heading angle change, then the travel distance is $L_{i,1} + L_{i,2}$, and the scaled increase $D_{p,i}$ in the travel distance is

$$D_{p,i} = (L_{i,1} + L_{i,2})/D_i. \tag{17}$$

The next step is to establish a relationship between the change in the heading angle and the resulting increase in fuel cost. Substituting the heading change $d\theta_i$ for $L_{i,1}$ in (17) and applying the law of cosines to solve for $L_{i,2}$ over the range $d\theta_i \in (-\pi/2, \pi/2)$, $D_{p,i}$ can be represented as

$$D_{p,i}(d\theta_i) = \frac{\frac{d_{i,1}}{\cos(d\theta_i)} + \sqrt{\left(\frac{d_{i,1}}{\cos(d\theta_i)}\right)^2 + D_i^2 - 2d_{i,1}D_i}}{D_i} \tag{18}$$

where the first term in the numerator corresponds to $L_{i,1}$, and the second term is $L_{i,2}$.

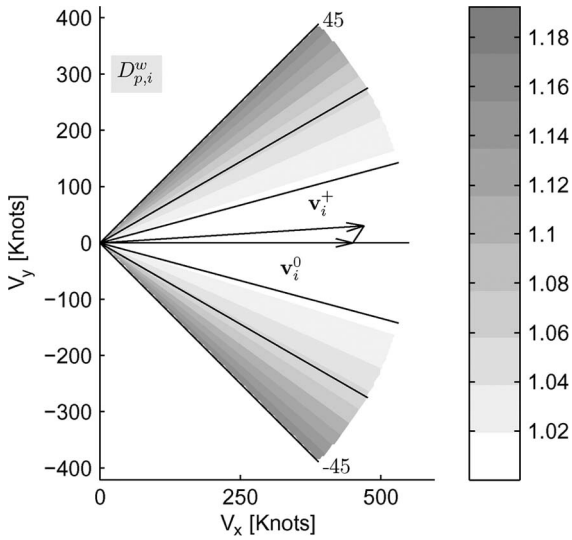

Fig. 7. Contour plot of the scaled additional distance traveled for a required heading change.

Assuming that any heading angle change allows for the aircraft to fly near the optimal fuel burn speed, the additional distance traveled according to relation (18) can be assumed to be equal to a fuel consumption measure. We then develop a tight linear approximation of the relation in (18). Note that (18) is a convex function in the interval $d\theta_i \in (-\pi/4, \pi/4)$, yet nonconvex in the decision variables $\mathbf{dv}_i$. A contour plot of $D_{p,i}$ as a function of the airspeed changes $\mathbf{dv}_i$ is given in Fig. 7. Thus, a linear approximation is possible by fitting a set of $2q$ planes between angles $[\theta_{-q}, \ldots, \theta_0, \ldots, \theta_q]$ to (18). Each plane w, approximating function (18) within some interval $[\theta_w, \theta_{w+1}]$, can be determined by first calculating the points x_w, y_w, z_w and $x_{w+1}, y_{w+1}, z_{w+1}$ as follows:

$$\begin{aligned} x_w &= v_{i,\max}\cos(\theta_w) \\ y_w &= v_{i,\max}\sin(\theta_w) \\ z_w &= D_{p,i}(\theta_w) \\ x_{w+1} &= v_{i,\max}\cos(\theta_{w+1}) \\ y_{w+1} &= v_{i,\max}\sin(\theta_{w+1}) \\ z_{w+1} &= D_{p,i}(\theta_{w+1}). \end{aligned} \tag{19}$$

Then, a linear function relating the scaled increase in distance traveled due to a heading deviation $d\theta_i$, where $d\theta_i \in [\theta_w, \theta_{w+1}]$, can be obtained from

$$\det\left(\begin{bmatrix} x & y & \hat{D}_{p,i}^w - 1 \\ x - x_w & y - y_w & \hat{D}_{p,i}^w - z_w \\ x - x_{w+1} & y - y_{w+1} & \hat{D}_{p,i}^w - z_{w+1} \end{bmatrix}\right) = 0 \tag{20}$$

where $\hat{D}_{p,i}^w$ is the approximate percent increase in distance traveled, $x = v_{i,x}^+$, and $y = v_{i,y}^+$. Note that relation (20) is a direct result of the points (x_w, y_w, z_w), $(x_{w+1}, y_{w+1}, z_{w+1})$, and $(x, y, \hat{D}_{p,i}^w)$ being on the same plane. The resulting relation can be included as a constraint in the optimization model as

$$\hat{D}_{p,i}^w = c_1 x + c_2 y + c_3 \tag{21}$$

where c_1, c_2, and c_3 are constants obtained from (20).

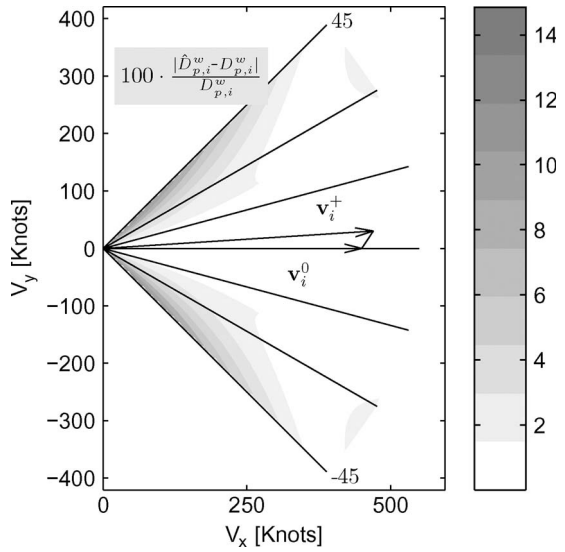

Fig. 8. Percent error in the approximation of the scaled additional distance traveled for a required heading change.

As shown in Fig. 8, the convex planar representation closely approximates $D_{p,i}(d\theta_i)$, where the approximation error is less than 1% for most values of the heading angle change within the nominal operating bounds.

Assuming that the aircraft operates at the optimal fuel burn rate when applying a heading change, the additional percentage fuel cost due to the heading angle change for the ith aircraft, i.e., u_i, over the optimal fuel burn rate is equal to the additional percentage of distance traveled, i.e., $D_{p,i}$. Hence, to implement the plane approximation in the optimization model, the following constraint to define the heading change costs u_i for each aircraft is included in the formulation:

$$\hat{D}^w_{p,i} \le u_i \qquad \forall\, w. \tag{22}$$

C. Total Cost Function

We assume that the overall objective is a mixture of the minimization of the sum of individual fuel costs, i.e., t_{sum}, and the minimization of the maximum fuel burn over all the aircraft, i.e., $t_{\max}$ (to ensure that no single aircraft is excessively penalized). Note that the individual fuel costs are equal to the sum of the costs that are incurred due to the change in airspeed t_i and the costs due to the change in heading angle u_i. Thus, the overall objective function for the problem can be expressed as

$$f_{\text{fuel}} = J_m t_{\max} + J_s t_{\text{sum}} \tag{23}$$

where J_m and J_s are constants that form a ratio for valuing the minmax or cumulative sum approaches and can be determined based on the policy that the decision maker wants to implement. The variables t_{sum} and $t_{\max}$ are defined in the formulation through the following sets of constraints:

$$\begin{aligned} t_i + u_i &\le t_{\max} \qquad \forall\, i \\ t_{\text{sum}} &= \sum_{i=1}^{n} (t_i + u_i). \end{aligned} \tag{24}$$

V. Model Summary and Implementation

The described optimization model can be implemented by formulating the problem through the objective function and the constraints described in Sections II–IV, as shown by the following:

$$\begin{aligned}
\min \quad & J_m t_{\max} + J_s t_{\text{sum}} \\
\text{s.t.} \quad & \\
\tilde{v}_{i,j,y} - \tilde{v}_{i,j,x} m^n_{i,j} &\le \left(1 - r^{ij}_1\right) M^{ij}_1 \qquad \forall\, i < j \\
-\tilde{v}_{i,j,x} &\le \left(1 - r^{ij}_1\right) M^{ij}_1 \qquad \forall\, i < j \\
-\tilde{v}_{i,j,y} + \tilde{v}_{i,j,x} m^p_{i,j} &\le \left(1 - r^{ij}_2\right) M^{ij}_2 \qquad \forall\, i < j \\
-\tilde{v}_{i,j,x} &\le \left(1 - r^{ij}_2\right) M^{ij}_2 \qquad \forall\, i < j \\
\tilde{v}_{i,j,x} &\le \left(1 - r^{ij}_3\right) M^{ij}_3 \qquad \forall\, i < j \\
\hat{D}^w_{p,i} &= c^i_1 v^+_{i,x} + c^i_2 v^+_{i,y} + c^i_3 \qquad \forall\, i \\
\tilde{v}_{i,j,x} &= v^{+,r}_{i,x} - v^{+,r}_{j,x} \qquad \forall\, i < j \\
\tilde{v}_{i,j,y} &= v^{+,r}_{i,y} - v^{+,r}_{j,y} \qquad \forall\, i < j \\
\mathbf{R}(\omega_{i,j}) &= \begin{bmatrix} \cos(\omega_{i,j}) & \sin(\omega_{i,j}) \\ -\sin(\omega_{i,j}) & \cos(\omega_{i,j}) \end{bmatrix} \qquad \forall\, i < j \\
\mathbf{v}^{+,r}_i &= \mathbf{R}(\omega_{i,j}) \mathbf{v}^+_i \qquad \forall\, i < j \\
\mathbf{v}^{+,r}_j &= \mathbf{R}(\omega_{i,j}) \mathbf{v}^+_j \qquad \forall\, i < j \\
a_{l,i} s_i + b_{l,i} &\le t_i \qquad \forall\, l, i \\
t_i + u_i &\le t_{\max} \qquad \forall\, i \\
t_{\text{sum}} &= \sum_{i=1}^{n} (t_i + u_i) \\
\sum_{k=1}^{3} r^{ij}_k &= 1 \qquad \forall\, i < j \\
v^+_{i,x} &= \sum_{q=0}^{m} X_q \lambda_q \qquad \forall\, i \\
v^+_{i,y} &= \sum_{q=0}^{m} Y_q \lambda_q \qquad \forall\, i \\
s_i &= \sum_{q=0}^{m} Z_q \lambda_q \qquad \forall\, i \\
\hat{D}^w_{p,i} &\le u_i \qquad \forall\, w, i \\
\sum_{q=0}^{m} \lambda_q &= 1 \\
r^{ij}_k &\in \{0,1\} \qquad \forall\, k, i < j \\
s_i, t_i, u_i, t_{\max}, t_{\text{sum}}, \hat{D}^w_{p,i} &\ge 0 \\
\lambda_q &\in \text{SOS2} \qquad \forall\, q
\end{aligned} \tag{25}$$

where arbitrarily large values can be selected for M^{ij}_k. However, tighter bounds on M^{ij}_k ensure efficient solutions by preventing excessive branching in the solver. Also, note that the binary variables r^{ij}_k model the either–or conditions in the separation constraints and serve as indicators for constraints that are enforced. Hence, the variables r^{ij}_k, along with the SOS2 variables λ_q, are auxiliary variables in the formulation. As

noted previously, both the objective function and the constraints in the problem are linear functions of the decision variables, and, thus, the resulting problem is a mixed-integer linear-programming model, which can be solved with any integer-programming solver.

One important question for a given instance of the problem might be whether a feasible solution exists for that instance. For a large number of aircraft and given constraints on aircraft dynamics, such as maximum and minimum heading and speed changes, it is not likely that solvability can be predetermined without initiating the optimization procedure. One special case where feasibility is ensured is when aircraft are allowed to make 90° heading changes, and all aircraft in the same flight level are traveling in the same direction, i.e., strictly east or west, as required by the Federal Aviation Administration. However, this may yield aggressive maneuvers and is outside of the scope of en route traffic. On the other hand, for most instances, infeasibility can be determined with reasonable efficiency through the implementation of the branch-and-bound procedure that is used in the optimization.

Another issue of interest involves the solvability of the model when one or more of the aircraft involved in the conflict are not able to maneuver. In such a situation, the existence of a feasible solution can still be determined in near real time by initiating the optimization algorithm. Indeed, the computational time that is required to identify infeasibility will typically be much less than the time required to solve the problem to optimality. Furthermore, if feasible solutions exist for this restricted case, the optimal solution can generally be obtained faster than the unrestricted case due to the reduced search space. In a related study, Vela *et al.* [19] consider conflict-resolution models where the optimization involves the minimization of the total number of maneuvers that are performed to resolve conflict.

VI. Computational Results

The performance of the proposed model has been tested with randomly generated test problems in a fixed area and with scenarios based on current air-traffic conditions. The first set of randomly generated test problems was used to analyze the computational complexity of the algorithm, i.e., the speed and the ability of the algorithm to find an optimal solution. The second set of simulations focused on establishing the cost performance of the algorithm in managing traffic within an en route airspace.

The computational complexity of the random models was assessed according to the number of planes involved and the density of the aircraft. Several different configurations were considered for the two complexity indexes. The 30 configurations are listed in Table I. The test problem configuration is indicated as follows: The number following the letter N represents the number of aircraft, while the number after the letter D is the length in nautical miles of a side of the square area that is considered for the problem. The instances were generated by randomly positioning the aircraft in the considered area according to an approximately uniform distribution. Cases in which the random sampling resulted in aircraft initially overlapping or within 10 nmi of each other were not considered.

TABLE I
Performance of the Proposed Approach on the Random Test Cases

Configuration	Avg. Solution Time (sec)	Avg. Optimality Gap (%)
N2D350	0.01	-
N2D300	0.01	-
N2D250	0.01	-
N2D200	0.01	-
N2D150	0.00	-
N5D350	0.03	-
N5D300	0.03	-
N5D250	0.03	-
N5D200	0.03	-
N5D150	0.03	-
N10D350	0.33	-
N10D300	0.38	-
N10D250	0.35	-
N10D200	0.33	-
N10D150	0.36	-
N15D350	8.93	0.01
N15D300	7.20	0.01
N15D250	8.57	0.05
N15D200	15.04	0.04
N15D150	9.94	0.02
N20D350	60.33	0.10
N20D300	60.07	0.10
N20D250	68.22	0.20
N20D200	73.58	0.40
N20D150	75.79	0.98
N25D350	81.09	1.44
N25D300	84.99	1.70
N25D250	86.51	2.87
N25D200	89.21	7.58
N25D150	89.25	12.45

The initial aircraft headings were randomly selected from a uniform distribution such that the aircraft fly within a 90° angle toward the center of the area. Each of the test instances assumes a minimum separation requirement of $d = 5$ nmi. Also, for all computational tests performed, the values used for J_m and J_s were 0 and 1, respectively.

Note that the computational complexity of the problem instances is not described by the number of conflicts, but rather by the number of pairwise constraints that are considered as part of the optimization procedure, which is a direct function of the number of aircraft in the problem. This computational complexity measure is used because the number of variables and constraints will have the most important impact in the computational performance of the algorithm. The only exception occurs with extreme situations where only a very small subset of aircraft is involved in conflicts. Furthermore, all aircraft must be considered in the problem to ensure no secondary conflicts arise.

Computations were performed with four parallel 2-GHz processors and 3 GB of total internal memory, using ILOG CPLEX Version 10.0. The algorithmic procedures available in ILOG CPLEX for SOS2 and indicator variables were utilized in the computational studies. For each of the 30 configurations, 40 random test problems were developed and solved. A stopping time of 90 s was used for the calculations, and the resulting average optimality gap and solution time for each configuration are reported in Table I.

Overall, the computational results from the randomly generated models show that the developed procedure is effective

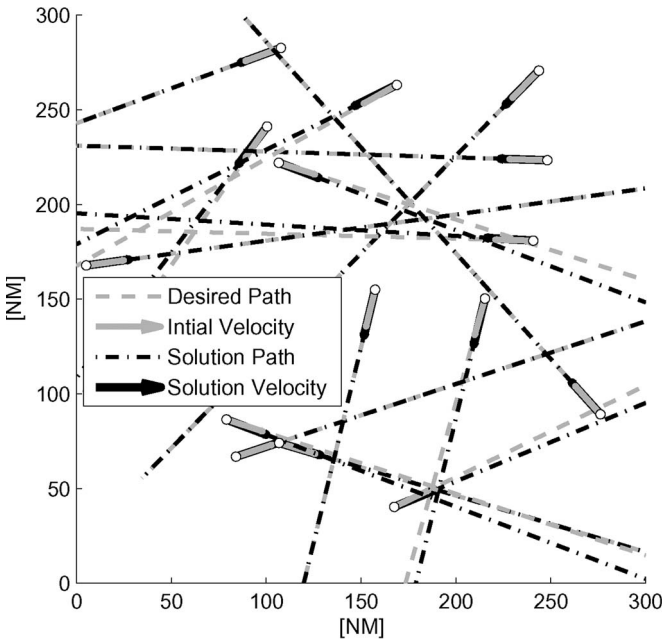

Fig. 9. Heading angle and speed changes required for the resolution of conflicts for a sample problem involving 15 aircraft.

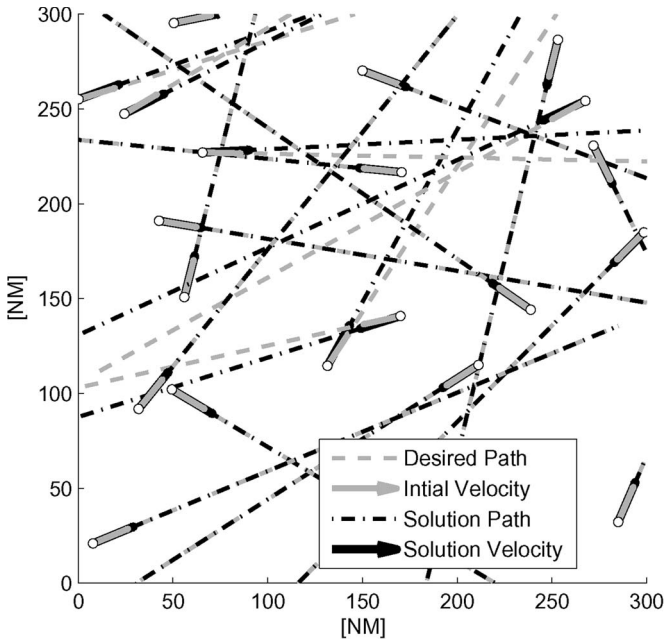

Fig. 10. Heading angle and speed changes required for the resolution of conflicts for a sample problem involving 20 aircraft.

and efficient in solving the conflict-resolution problem in near real time, even for situations with a relatively large number of aircraft in the airspace. The solution times start to substantially increase as the number of aircraft exceeds 15, which rarely occurs in actual air-traffic flow. However, for instances where there are 15 or more aircraft, the proposed approach is still able to produce very good feasible conflict-resolution procedures in 90 s or less; the average optimality gap, which measures the percent difference between the best estimated lower bound and the best solution obtained at the termination of the algorithm, remains low. Therefore, in a real-time implementation, a near-optimal solution can still be obtained if time limitations allow only a short time for optimization. Note that all pairs of aircraft are simultaneously resolved, regardless of the likelihood of a possible conflict, and the algorithm does not make use of any heuristics to reduce the complexity. Hence, the computation limitation and the problem difficulty arise from the optimization solver's ability to iterate through the branch-and-bound tree.

Figs. 9 and 10 show the heading angle and speed changes that are required for the resolution of conflicts for sample problems involving 15 and 20 aircraft, respectively. These examples demonstrate the solutions from the algorithm by displaying the original heading and velocity information for each aircraft, as well as the revised heading and velocity suggested by the solution. In most cases, the changes are minimal, showing that the deviation from optimal fuel consumption is as small as possible.

The second set of computational tests involved the implementation of the model in a realistic setting based on current air-traffic patterns in the Cleveland Center. Traffic levels up to twice the current peak levels were used in the simulations to demonstrate the capability that the proposed algorithm can be implemented in real operational situations. In addition to a direct implementation of the algorithm, additional tests were also conducted where only speed changes were allowed for conflict resolution. These realistic tests were dynamically conducted in a receding horizon format to simulate directing traffic through the Cleveland Center. The conflict-resolution problem was solved each time a new aircraft entered the air space over a 5-h period. Because the conflict-resolution problem is resolved in a continuous manner, it allows for any aircraft that have made heading or speed changes to return toward their original destination or to return to their desired airspeed after clearing a conflict.

To approximate traffic through the center, a statistical distribution of entry–exit pairs was generated using historical data of aircraft traveling through the center at and above FL300 during the 24-h period of May 1, 2005. The date selected represents a nominal day in the National Airspace System with no significant disruptions. The center boundary was broken up into 10-nmi segments, which were numerically identified for entrances and exits. For the distribution, each aircraft was designated to enter and exit through a particular boundary segment. Aircraft interarrival times into the center were assumed to follow an exponential distribution with a slight modification such that aircraft entering at the same entrance had a minimum time separation of 2 min.

To increase traffic loads, the average interarrival time between aircraft was decreased. Aircraft models were also assigned according to a sampled distribution that was taken from historical data. The aircraft span a broad range, including regional, narrow-body, wide-body, and business-class jets. For the purpose of simulation, all sampled aircraft trajectories provided to the simulation were assumed to be flying east to west at FL360. An example of the sampled traffic pattern through the Cleveland Center is displayed in Fig. 11. The darker and thicker lines in the figure correspond to entry–exit pairs that are more frequently used in the simulation, which also correspond to the distributions that are calculated from historical data. The cost for each simulation was determined by calculating the sum of the ratio of the fuel cost for the resulting trajectory F_{sim} to the

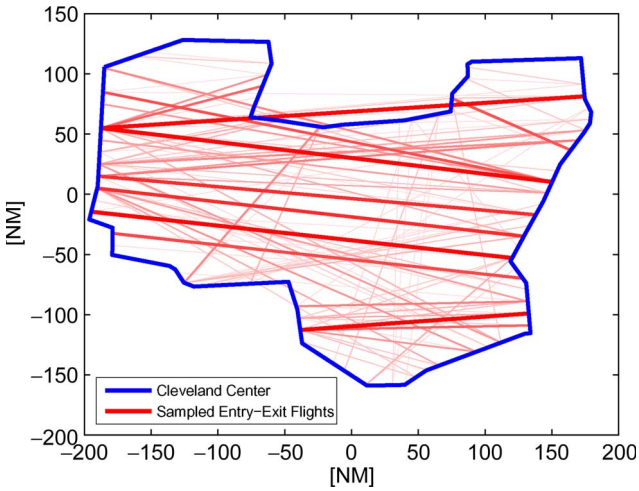

Fig. 11. Randomly generated flights in the Cleveland Center based on distributions calculated from historical data.

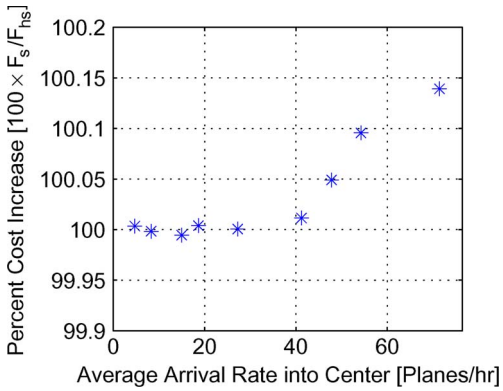

Fig. 12. Percent difference in cost when only speed changes are allowed.

minimum total fuel burn for each aircraft if they were directly routed from entrance to exit at their corresponding fuel optimal airspeed F_{direct}, i.e., $\sum_{i=1}^{n} F^i_{\text{sim}}/F^i_{\text{direct}}$.

The simulations were performed similar to a near real-time implementation, where the problem was solved multiple times based on the occurrence of new conflicts. A time limit of 90 s was used for each computation. In addition to the feasibility of real-time implementation, a comparison of the results from these tests demonstrates the savings that are gained by considering both heading and speed changes in a conflict resolution algorithm. Fig. 12 shows the percent increase in cost when only speed control is used to resolve conflicts. The peak capacity of the Cleveland Center at FL360 given by the number of aircraft in the airspace, according to historical data, was 25 aircraft, corresponding to an approximate arrival rate of 42 planes/h. In some instances, with a very few number of aircraft, the speed-only solution obtained at the end of the allocated time was slightly better. On the other hand, in high traffic instances, the speed-only problems were either infeasible or had solutions with larger costs. Therefore, while the improvement margins are small for levels that are below peak capacity, they clearly demonstrate an overall improvement, particularly as traffic levels increase. Additionally, allowing for simultaneous heading and speed changes clearly provides greater latitude in solving any conflict-resolution problem.

VII. Conclusion and Future Work

A new and advanced air-traffic conflict-resolution methodology has been presented. The major advancement in this paper is a methodology that allows for simultaneous aircraft heading and speed changes to resolve conflicts in near real time. The maneuvers have been determined such that the fuel costs incurred due to the changes are minimized. Furthermore, the nonconvex cost functions of airspeeds and headings have been modeled using linear approximations, which lead to very accurate representations of the actual cost functions. Moreover, most significantly, optimal conflict-resolution maneuvers of the proposed approach have been identified in only a few seconds. This enables implementation of the developed methodology in real-time traffic-flow management.

An important consideration in air-traffic-flow management is controller workload. Given the difficulty of modeling and estimation of the number/types of resolution commands to be issued by a human controller, a direct integration of the controller workload in an optimization-based conflict-resolution algorithm is not possible. One possible approach to approximate the controller workload can be by developing a parametric optimization framework, where the number and the types of resolution commands are restricted or penalized. The parameters of the model can then be calibrated to best represent human controllers' actions. Vela *et al.* [19] have taken some initial steps in developing such a parametric model.

The developed procedure can further be extended to three dimensions by modeling multiple flight levels and introducing new variables in the mixed-integer programming formulation. Each aircraft i will include a binary SOS variable of order 1 representing the feasible flight levels L_{il}, and each pair of aircraft i and j requires a binary variable $L^d_{i,j}$ to indicate if the aircraft are traveling at different flight levels. The value of L_{il} is 1 when aircraft i operates at flight level l. Hence, aircraft traveling along the same flight levels, i.e., $L^d_{i,j} = 0 \leftrightarrow L_{il} + L_{jl} = 2$, will require conflict resolution, and the separation constraints described in Section III will need to be enforced only for aircraft pairs i and j if $L^d_{i,j} = 0$. These conditions can be integrated into the model by using classical "if–then" type constraint constructs in integer programming [20]. Details of such an extended model are described in another paper by Vela *et al.* [21], where problem formulations and some computational results are presented.

Furthermore, the model can be compared with existing heuristic procedures, and the results from the fully implemented optimization procedure can be used as a baseline in evaluating other proposed methods. In addition, computational performance for instances involving a very large number of aircraft can be improved by using different parallelization schemes and advanced integer programming solution techniques.

Appendix
Derivation of Separation Constraints

The mathematical derivation of the separation constraints involves an extension of (1) through various substitutions and algebraic manipulations. The general process consists of determining the minimum separation between two aircraft for $t > 0$

as a function of the relative velocities and, thereby, defining tight constraints on the velocities to ensure minimum separation. As can be observed in Fig. 3, this can be achieved through geometric principles such as the shortest distance between a point and a line being the perpendicular between the point and the line and the scaling of similar triangles.

Consider any pair of aircraft rotated such that the angle between the horizon and the connector between aircraft is 0°, as shown in Fig. 2. From inequality (1), it is required that

$$\sqrt{x_{\text{dist}}^2 + y_{\text{dist}}^2} \geq d_{i,j}^{\min} \qquad \forall\, t \in R^+.$$

Because the separation condition (1) is invariant to the rotation of the space through the linear transformation in (5), x_{dist} and y_{dist} can be replaced by x_{dist}^r and y_{dist}^r in the new coordinate frame, i.e.,

$$\begin{aligned} x_{\text{dist}}^r &= \left(x_i^r + v_{i,x}^r t\right) - \left(x_j^r + v_{j,x}^r t\right) \\ y_{\text{dist}}^r &= \left(y_i^r + v_{i,y}^r t\right) - \left(y_j^r + v_{j,y}^r t\right). \end{aligned} \tag{26}$$

Maintaining notation, the distance between the aircraft can be expressed in terms of the relative coordinates, i.e.,

$$d_{i,j} = \sqrt{\left(\tilde{\mathbf{v}}_{i,j,x} t + \tilde{\mathbf{p}}_{i,j,x}\right)^2 + \left(\tilde{\mathbf{v}}_{i,j,y} t + \tilde{\mathbf{p}}_{i,j,y}\right)^2}. \tag{27}$$

It is clear that in the rotated frame, $\tilde{\mathbf{p}}_{i,j,y} = 0$ and $\tilde{\mathbf{p}}_{i,j,x} = \|p_i - p_j\| = D$, which, after substituting into (27) and expanding, leads to

$$d_{i,j} = \sqrt{\left(\tilde{\mathbf{v}}_{i,j,x}^2 + \tilde{\mathbf{v}}_{i,j,y}^2\right) t^2 + 2t(D\tilde{\mathbf{v}}_{i,j,x}) + D^2}. \tag{28}$$

For aircraft pairs i and j such that $\tilde{\mathbf{v}}_{i,j,x} \leq 0$, indicating that the aircraft are moving away from each other, the separation distance between the aircraft is nondecreasing with time. Hence, since initial conditions require $D \geq d_{i,j}^{\min}$, the pair of aircraft will never break the separation condition (1). The last constraint in (10) is a direct result of this analysis.

For the case when $\tilde{\mathbf{v}}_{i,j,x} \geq 0$, a more detailed derivation is required. The first task requires finding the minimum separation of the aircraft as a function of $\tilde{\mathbf{v}}_{i,j,x}$ and $\tilde{\mathbf{v}}_{i,j,y}$ by taking the derivative (28) in terms of time t. Solving for t, the time corresponding to the minimum distance is

$$t^{\min} = \frac{-D\tilde{\mathbf{v}}_{i,j,x}}{\tilde{\mathbf{v}}_{i,j,x}^2 + \tilde{\mathbf{v}}_{i,j,y}^2}. \tag{29}$$

When $t^{\min}$ is substituted back into (28), the corresponding minimum distance between the aircraft for a given $\tilde{\mathbf{v}}_{i,j,x}$ and $\tilde{\mathbf{v}}_{i,j,y}$ is

$$d_{i,j}|_{t^{\min}} = D\left[\frac{\tilde{\mathbf{v}}_{i,j,y}^2}{\tilde{\mathbf{v}}_{i,j,x}^2 + \tilde{\mathbf{v}}_{i,j,y}^2}\right]^{1/2} \geq d_{i,j}^{\min} \qquad \forall\, t \in R^+. \tag{30}$$

Through a sequence of algebraic manipulations, an inequality between $\tilde{\mathbf{v}}_{i,j,x}$ and $\tilde{\mathbf{v}}_{i,j,y}$ can be identified as follows:

$$D^2\left[\frac{\tilde{\mathbf{v}}_{i,j,y}^2}{\tilde{\mathbf{v}}_{i,j,x}^2 + \tilde{\mathbf{v}}_{i,j,y}^2}\right] \geq \left(d_{i,j}^{\min}\right)^2 \tag{31}$$

$$D^2\left(\tilde{\mathbf{v}}_{i,j,y}^2\right) \geq \left(\tilde{\mathbf{v}}_{i,j,x}^2 + \tilde{\mathbf{v}}_{i,j,y}^2\right)\left(d_{i,j}^{\min}\right)^2 \tag{32}$$

$$\left[D^2 - \left(d_{i,j}^{\min}\right)^2\right]\tilde{\mathbf{v}}_{i,j,y}^2 \geq \tilde{\mathbf{v}}_{i,j,x}^2\left(d_{i,j}^{\min}\right)^2 \tag{33}$$

$$\tilde{\mathbf{v}}_{i,j,y}^2 \geq \tilde{\mathbf{v}}_{i,j,x}^2 \frac{\left(d_{i,j}^{\min}\right)^2}{D^2 - \left(d_{i,j}^{\min}\right)^2}. \tag{34}$$

The remaining two constraint equations in (10) are immediate from the results in (34). Given $\tilde{\mathbf{v}}_{i,j,x} \geq 0$, the inequality can then be expressed as two sets of linear inequalities, i.e.,

$$\begin{aligned} &\tilde{\mathbf{v}}_{i,j,y} \geq \tilde{\mathbf{v}}_{i,j,x} \frac{d_{i,j}^{\min}}{\sqrt{D^2 - \left(d_{i,j}^{\min}\right)^2}}, \qquad \tilde{v}_{i,j,x} \geq 0 \\ \text{or} \quad &\tilde{\mathbf{v}}_{i,j,y} \leq -\tilde{\mathbf{v}}_{i,j,x} \frac{d_{i,j}^{\min}}{\sqrt{D^2 - \left(d_{i,j}^{\min}\right)^2}}, \qquad \tilde{v}_{i,j,x} \geq 0. \end{aligned} \tag{35}$$

ACKNOWLEDGMENT

The authors would like to thank A. Abad of the Department of Aeronautics and Astronautics, Massachusetts Institute of Technology, Cambridge, for his assistance in the initial stages of this paper with understanding the approach taken in [14].

REFERENCES

[1] J. Kuchar and L. Yang, "A review of conflict detection and resolution modeling methods," *IEEE Trans. Intell. Transp. Syst.*, vol. 1, no. 4, pp. 179–189, Dec. 2000.

[2] H. Erzberger, "Automated conflict resolution for air traffic control," in *Proc. Int. Congr. Aeronautical Sci.*, 2006, pp. 1–27.

[3] T. Farley, M. Kupfer, and H. Erzberger, "Automated conflict resolution: A simulation evaluation under high demand including merging arrivals," presented at the AIAA Aviation Technol., Integration Operation Conf., Belfast, Northern Ireland, 2007, Paper AIAA 2007-7736.

[4] J. Goss, R. Rajvanshi, and K. Sabarrao, "Aircraft conflict detection and resolution using mixed geometric and collision cone approaches," presented at the AIAA Guidance, Navigation, Control Conf. Exhibit, Providence, RI, 2004, Paper AIAA 2004-4879.

[5] J. Hu, M. Prandini, and S. Sastry, "Optimal coordinated maneuvers for three dimensional aircraft conflict resolution," in *J. Guid., Control Dyn.*, Sep./Oct. 2002, vol. 25, no. 5, pp. 888–900.

[6] K. Bilimoria and H. Lee, "Aircraft conflict resolution with an arrival time constraint," presented at the AIAA Guidance, Navigation, Control Conf. Exhib., Monterey, CA, 2002, Paper AIAA 2002-4444.

[7] S. Mondoloni and S. Conway, "An airborne conflict resolution approach using a genetic algorithm," Nat. Aeronautics Space Admin., Washington, DC, Tech. Rep. NASA-AIAA-2001-4054, 2001.

[8] R. Vivona, D. Karr, and D. Roscoe, "Pattern based genetic algorithm for airborne conflict resolution," presented at the AIAA Guidance, Navigation, Control Conf. Exhib., Keystone, CO, 2006, Paper AIAA 2006-6060.

[9] H. Idris, T. Hsu, and R. Vivona, "Time based conflict resolution algorithm and application to descent conflicts," presented at the AIAA Guidance, Navigation, Control Conf. Exhib., Austin, TX, 2003, Paper AIAA 2003-5517.

[10] D. Kirk, W. Heagy, and M. Yablonski, "Problem resolution support for free flight operations," *IEEE Trans. Intell. Transp. Syst.*, vol. 2, no. 2, pp. 72–80, Jun. 2001.

[11] A. Bicchi and L. Pallottino, "On optimal cooperative conflict resolution for air traffic management systems," *IEEE Trans. Intell. Transp. Syst.*, vol. 1, no. 4, pp. 221–231, Dec. 2000.
[12] S. Wollkind, J. Valasek, and T. Ioerger, "Automated conflict resolution for air traffic management using cooperative multiagent negotiation," presented at the AIAA Guidance, Navigation, Control Conf. Exhib., Providence, RI, 2004, Paper AIAA-2004-4992.
[13] C. Tomlin, I. Mitchell, and R. Ghosh, "Safety verification of conflict resolution maneuvers," *IEEE Trans. Intell. Transp. Syst.*, vol. 2, no. 2, pp. 110–120, Jun. 2001.
[14] L. Pallottino, E. M. Feron, and A. Bicchi, "Conflict resolution problems for air traffic management systems solved with mixed integer programming," *IEEE Trans. Intell. Transp. Syst.*, vol. 3, no. 1, pp. 3–11, Mar. 2002.
[15] W. Hylkema and H. Visser, "Aircraft conflict resolution taking into account controller workload using mixed integer linear programming," presented at the AIAA Guidance, Navigation, Control Conf. Exhib., 2003, Paper AIAA 2003-6726.
[16] M. Christodoulou and S. Kodaxakis, "Automatic commercial aircraft collision avoidance in free flight: The three dimensional problem," *IEEE Trans. Intell. Transp. Syst.*, vol. 7, no. 2, pp. 242–249, Jun. 2006.
[17] A. Nuic, "Aircraft performance summary tables for the base of aircraft data," Eurocontrol Experimental Center, Brussels, Belgium, Note No. 11/04, 2004.
[18] M. Gariel and E. Feron, "Graceful degradation of air traffic operations: Airspace sensitivity to degraded surveillance systems," *Proc. IEEE*, vol. 96, no. 12, pp. 2028–2039, Dec. 2008.
[19] A. Vela, S. Solak, E. Feron, K. Feigh, W. Singhose, and J.-P. Clarke, "A fuel optimal and reduced controller workload optimization model for conflict resolution," in *Proc. 28th Digital Avionics Syst. Conf.*, 2009, pp. 3.C.3-1–3.C.3-16.
[20] L. A. Wolsey, *Integer Programming*. New York: Wiley-Interscience, 1998.
[21] A. Vela, S. Solak, W. Singhose, and J. Clarke, "A mixed integer program for flight level assignment and speed control for conflict resolution," in *Proc. 48th IEEE Conf. Decision Control*, 2009, pp. 5219–5226.

Adan E. Vela received the B.S. degree from the University of California, Berkeley, in 2003 and the M.S. degree in mechanical engineering from Stanford University, Stanford, CA, in 2005. He is currently working toward the Ph.D. degree with the School of Mechanical Engineering, Georgia Institute of Technology, Atlanta, under the guidance of Dr. W. Singhose and coadvised by Dr. J.-P. Clarke within the School of Aerospace Engineering.

His research interests include the application of optimization for the control of robotic and air-traffic systems.

Senay Solak received the B.S. degree in electrical engineering from the United States Naval Academy, Annapolis, MD, in 1997 and the M.S. and Ph.D. degrees in industrial engineering from the Georgia Institute of Technology, Atlanta, in 2002 and 2007, respectively.

He is currently an Assistant Professor of operations management with the Isenberg School of Management, University of Massachusetts, Amherst, where he teaches and conducts research in the areas of optimization and simulation. His research focuses on applications of stochastic optimization in aviation, particularly in traffic-flow management and airspace capacity modeling.

John-Paul B. Clarke received the S.B., S.M., and Sc.D. degrees from the Massachusetts Institute of Technology, Cambridge, in 1991, 1992, and 1997, respectively.

He is currently an Associate Professor with the School of Aerospace Engineering and the Director of the Air Transportation Laboratory, Georgia Institute of Technology, Atlanta. His research and teaching address issues of optimization and robustness in aircraft and airline operations, air-traffic management, and the environmental impact of aviation.

William E. Singhose received the B.S. degree in mechanical engineering from the Massachusetts Institute of Technology (MIT), Cambridge, in 1990, the M.S. degree from Stanford University, Stanford, CA, in 1992, and the Ph.D. degree in mechanical engineering from MIT in 1997.

He is currently an Associate Professor with the School of Mechanical Engineering, Georgia Institute of Technology, Atlanta. His research focuses on the dynamics and control of flexible machines. He has developed numerous control schemes that alter the reference signals, resulting in vibration-free motion.

Earl R. Barnes received the B.S. degree from Morgan State College, Baltimore, MD, in 1964 and the Ph.D. degree from the University of Maryland, College Park, in 1968.

He is currently a Professor with the School of Industrial and Systems Engineering, Georgia Institute of Technology, Atlanta. His research interests include numerical methods for solving optimization problems. In particular, he is interested in interior point methods for linear programming problems and in nonlinear approaches to certain combinatorial optimization problems.

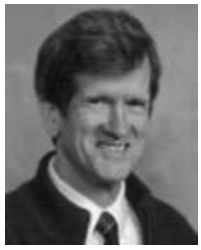

Ellis L. Johnson received the B.A. degree in mathematics from the Georgia Institute of Technology, Atlanta, and the Ph.D. degree in operations research from the University of California, Berkeley, in 1964.

He is currently the Coca-Cola Chaired Professor with the School of Industrial and Systems Engineering, Georgia Institute of Technology. His research interests include logistics, crew scheduling and real-time repair, fleet assignment and routing, distribution planning, network problems, and combinatorial optimization.